Некоторые результаты эксперимента LHAASO

Стенькин Ю.В.
ИЯИ РАН

A LARGE HIGH ALTITUDE AIR SHOWER OBSERVATORY

LHAASO PROJECT

(LHAASO Collaboration)

[1]Key Laboratory of Particle Astrophyics & Experimental Physics Division & Computing Center, Institute of High Energy Physics, Chinese Academy of Sciences, 100049 Beijing, China
[2]University of Chinese Academy of Sciences, 100049 Beijing, China
[3]TIANFU Cosmic Ray Research Center, Chengdu, Sichuan, China
[4]State Key Laboratory of Particle Detection and Electronics, China
[5]University of Science and Technology of China, 230026 Hefei, Anhui, China
[6]Department of Engineering Physics, Tsinghua University, 100084 Beijing, China
[7]National Astronomical Observatories, Chinese Academy of Sciences, 100101 Beijing, China
[8]National Space Science Center, Chinese Academy of Sciences, 100190 Beijing, China
[9]School of Physics, Peking University, 100871 Beijing, China
[10]Center for Astrophysics, Guangzhou University, 510006 Guangzhou, Guangdong, China
[11]School of Physics and Astronomy & School of Physics (Guangzhou), Sun Yat-sen University, 519000 Zhuhai, Guangdong, China
[12]School of Physical Science and Technology, Guangxi University, 530004 Nanning, Guangxi, China
[13]Hebei Normal University, 050024 Shijiazhuang, Hebei, China
[14]School of Physics and Microelectronics, Zhengzhou University, 450001 Zhengzhou, Henan, China
[15]School of Astronomy and Space Science, Nanjing University, 210023 Nanjing, Jiangsu, China
[16]Key Laboratory of Dark Matter and Space Astronomy, Purple Mountain Observatory, Chinese Academy of Sciences, 210023 Nanjing, Jiangsu, China
[17]Institute of Frontier and Interdisciplinary Science, Shandong University, 266237 Qingdao, Shandong, China
[18]Key Laboratory for Research in Galaxies and Cosmology, Shanghai Astronomical Observatory, Chinese Academy of Sciences, 200030 Shanghai, China
[19]Tsung-Dao Lee Institute & School of Physics and Astronomy, Shanghai Jiao Tong University, 200240 Shanghai, China
[20]School of Physical Science and Technology & School of Information Science and Technology, Southwest Jiaotong University, 610031 Chengdu, Sichuan, China
[21]College of Physics, Sichuan University, 610065 Chengdu, Sichuan, China
[22]Key Laboratory of Cosmic Rays (Tibet University), Ministry of Education, 850000 Lhasa, Tibet, China
[23]School of Physics and Technology, Wuhan University, 430072 Wuhan, Hubei, China
[24]School of Physics and Astronomy, Yunnan University, 650091 Kunming, Yunnan, China
[25]Yunnan Observatories, Chinese Academy of Sciences, 650216 Kunming, Yunnan, China
[26]Dublin Institute for Advanced Studies, 31 Fitzwilliam Place, 2 Dublin, Ireland
[27]Max-Planck-Institut for Nuclear Physics, P.O. Box 103980, 69029 Heidelberg, Germany
[28]Dipartimento di Fisica dell'Università di Napoli "Federico II", Complesso Universitario di Monte Sant'Angelo, via Cinthia, 80126 Napoli, Italy
[29]Institute for Nuclear Research of Russian Academy of Sciences, 117312 Moscow, Russia
[30]Moscow Institute of Physics and Technology, 141700 Moscow, Russia
[31]Département de Physique Nucléaire et Corpusculaire, Faculté de Sciences, Université de Genève, 24 Quai Ernest Ansermet, 1211 Geneva, Switzerland
[32]Department of Physics, Faculty of Science, Mahidol University, 10400 Bangkok, Thailand

Расположение: 4410 м над уровнем моря, восток Тибетского плато, Даоченг, Сычуань, КНР

Стенькин Ю.В. Зацепинские чтения 2023

Решаемые задачи

- What are the origins of cosmic rays?
  - Are the accelerators of hadrons different from electrons?
  - How high in energy can galactic sources produce particles?
  - What are the sources of the UHECRs?
- How do astrophysical sources accelerate particles?
  - What is the role of the extreme gravitational an magnetic fields surrounding black holes and neutron stars?
  - How are particles accelerated within relativistic jets?
  - Is there limit of the nature accelerators? What are they?
  - How do GRBs release so much energy in such a short time?
- How do CRs propagate inside/outside our galaxy?
  - What are origins of both “knees”?
- Fundamental physics & cosmology
  - What is the EBL and how did it evolve?
  - What is the dark matter?
  - What are the tightest constraints on Lorentz invariance?
  - Are there primordial black holes?
- Geophysical researches

Detector Layout in LHAASO

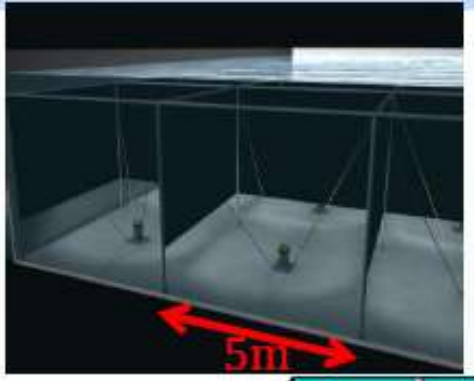

ENDA-400

MD

WFCTA

ED

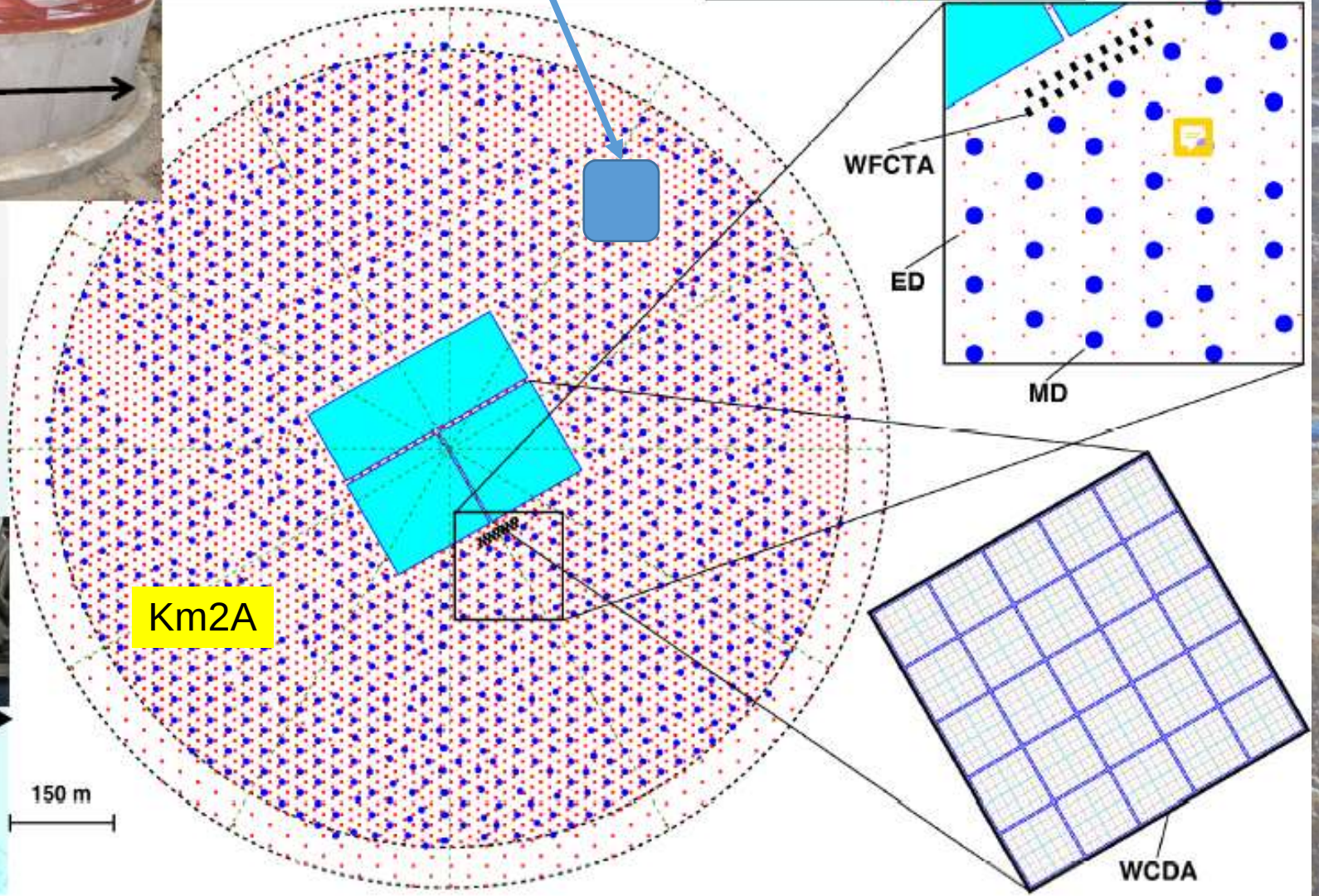

Km2A

MD

1188 MD

Именно эта установка первой начала получать выдающиеся результаты, благодаря огромной светосиле, большой плотности детекторов и качественной работе

En-detector

ED

5249 ED

Performance of ½ KM2A

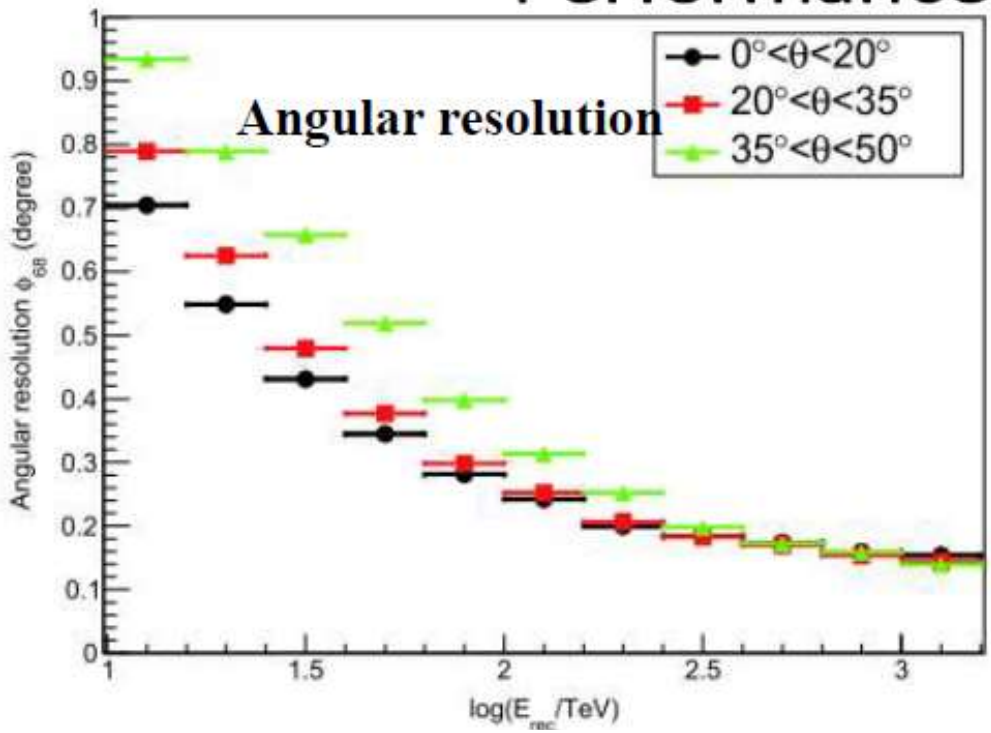

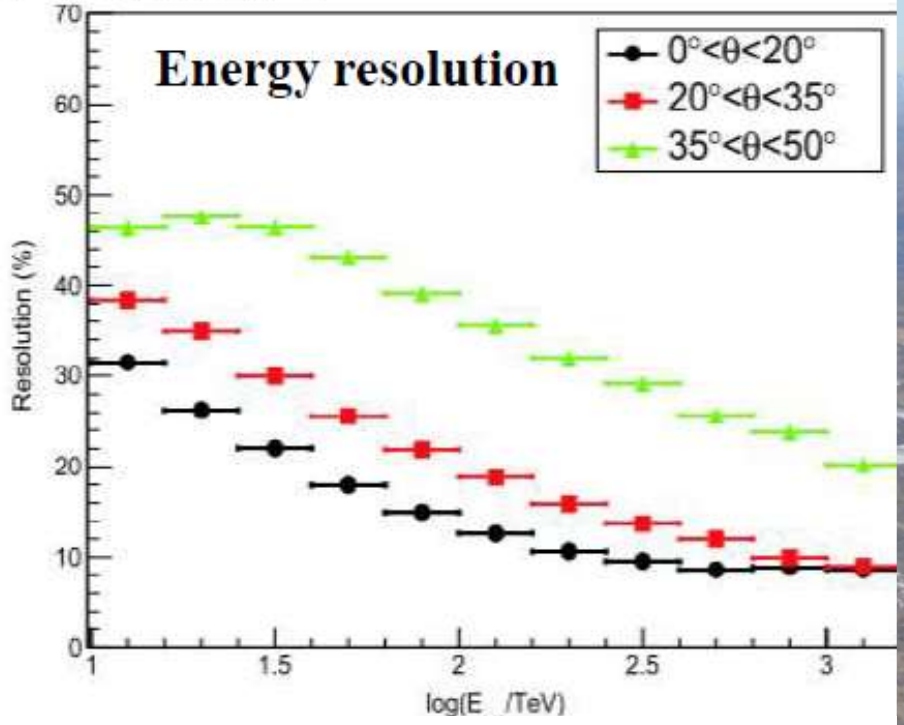

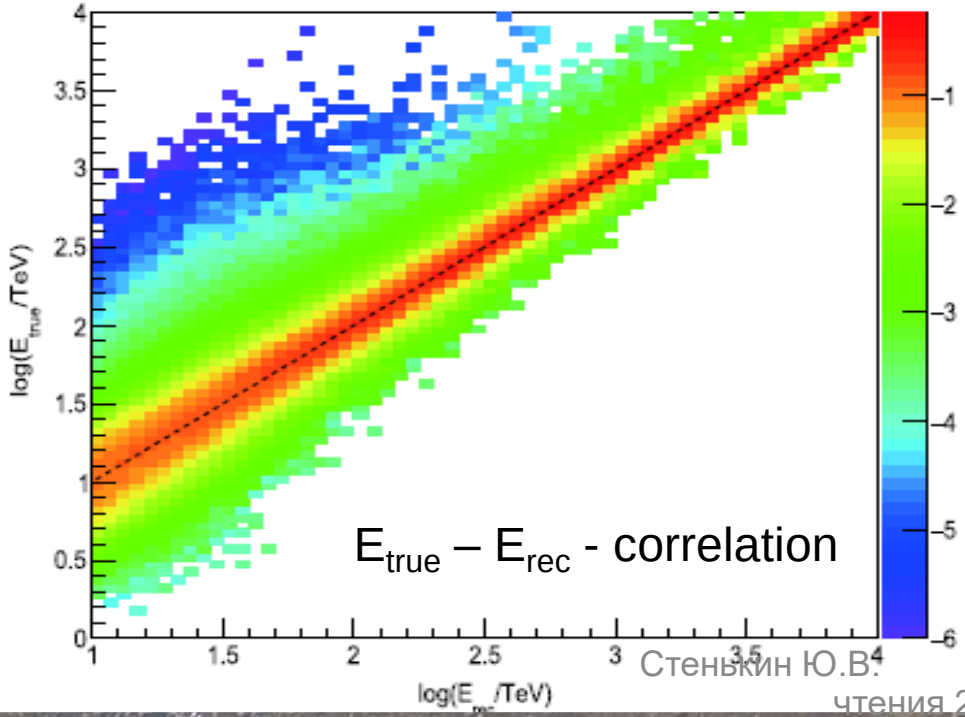

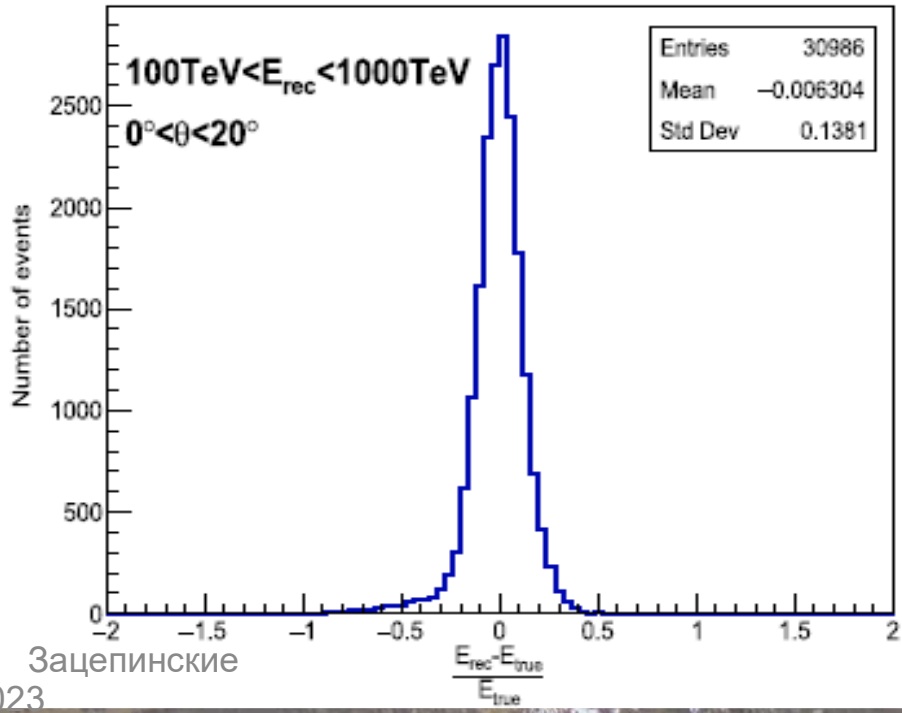

Отбор γ-ливней (по N_μ)

Chinese Physics C Vol. 45, No. 2 (2021)

Вероятность имитации протонным ливнем
< 10^{-4} при E >500 TeV

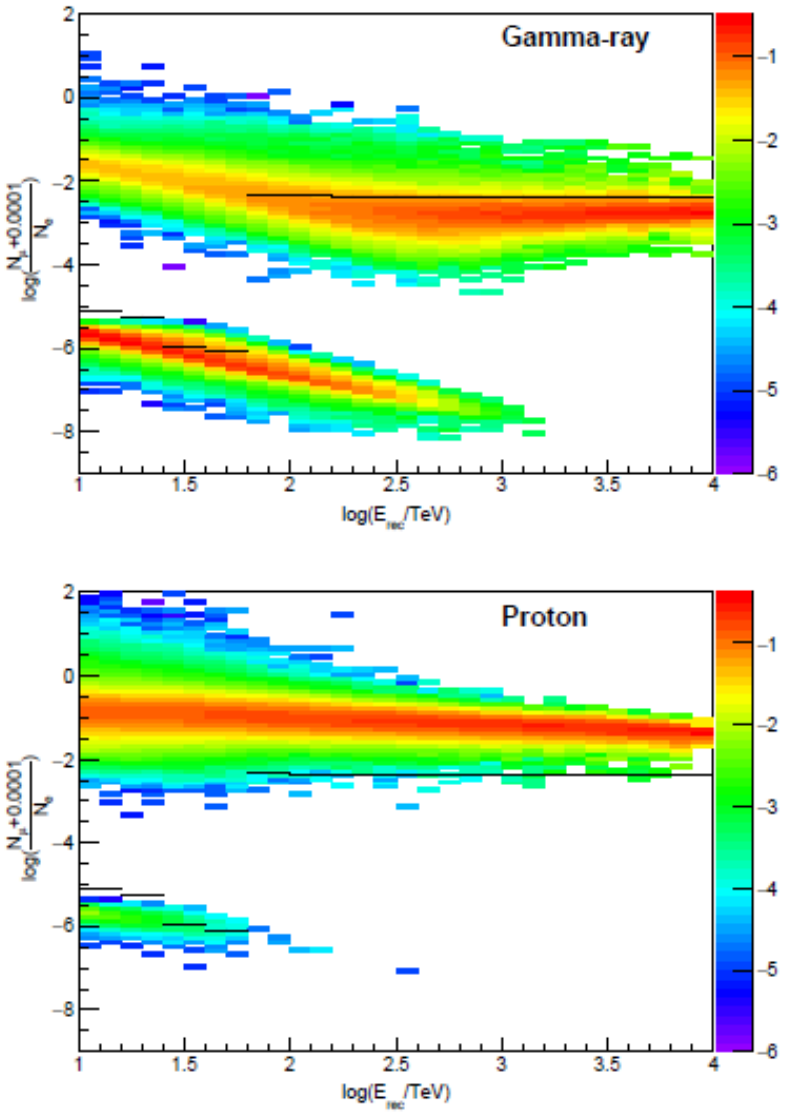

Fig. 9. Scatter plot of R as defined in equation (6) vs. reconstructed energy using simulated gamma-ray-induced (upper panel) and proton-induced (lower panel) air showers, respectively. The color represents the log probability density within each E_{rec} bin. The solid lines indicate the gamma-ray/background discrimination cuts used in this work.

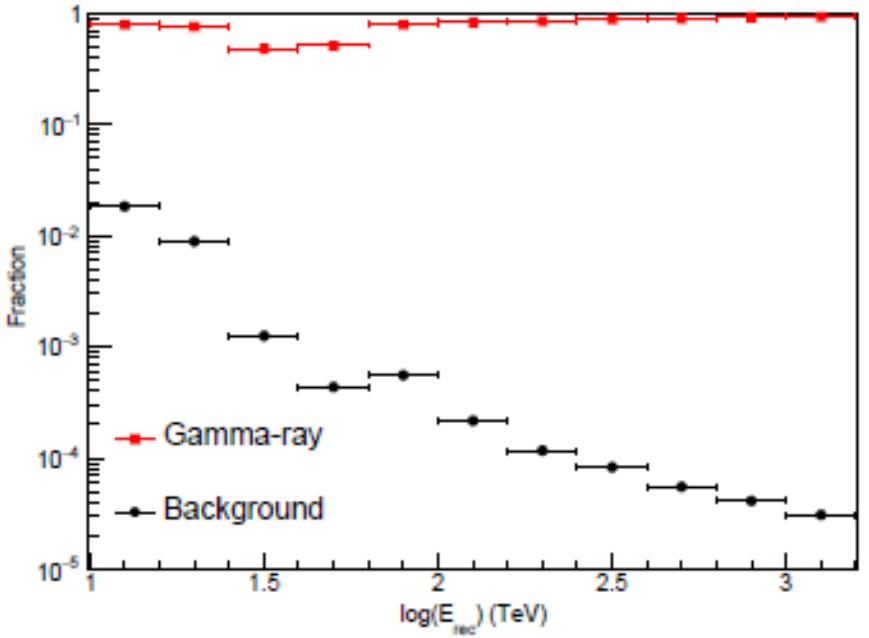

Fig. 10. The survival fraction of gamma-ray (according to simulation) and cosmic ray background events (according to observational data) in different energy bins after the discrimination cuts.

Краб в трех энергетических диапазонах

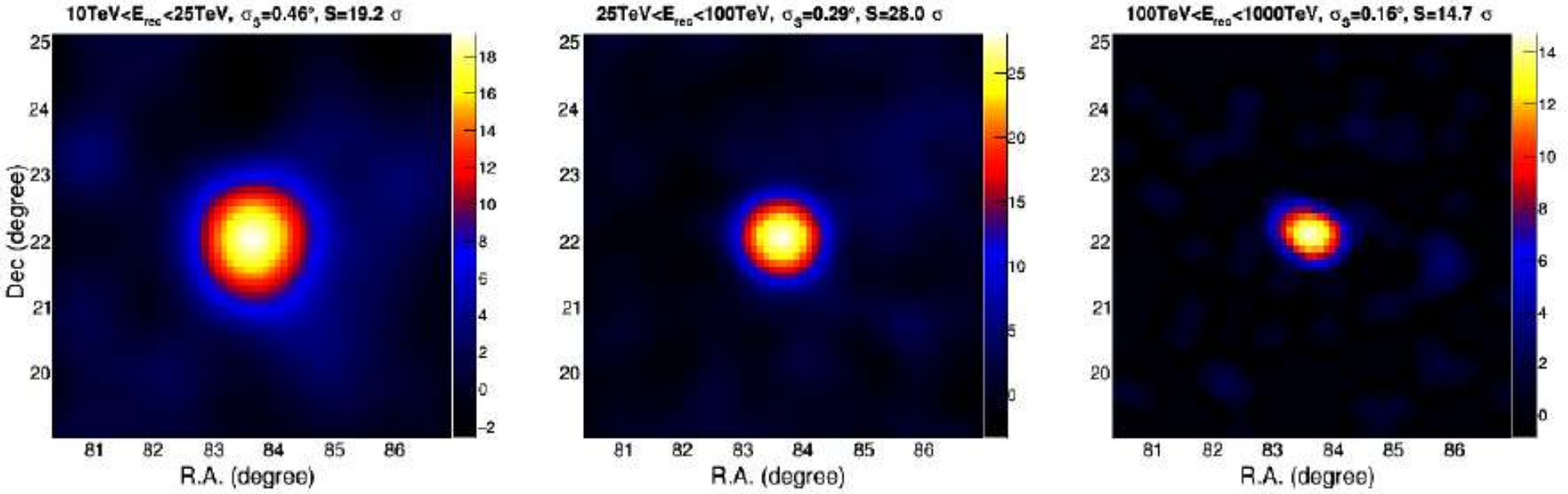

Fig. 14. Significance maps centered on the Crab Nebula at three energy ranges. σ_S is the sigma of the 2-dimension
or represents the significance. S is the maximum value in

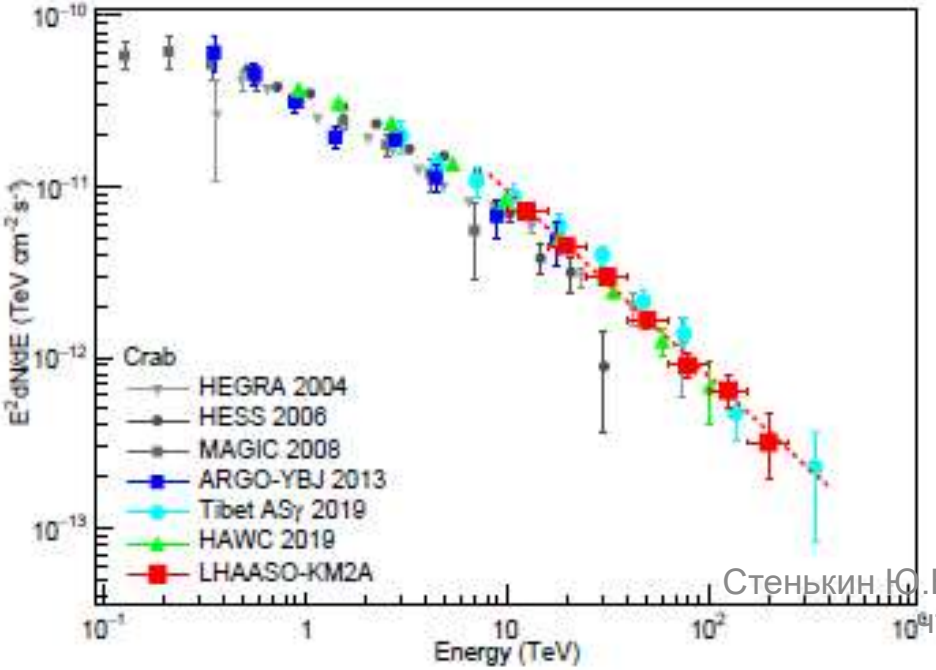

$$f(E) = (1.13 \pm 0.05_{stat} \pm 0.08_{sys}) \times 10^{-14} \left(\frac{E}{20TeV}\right)^{-3.09 \pm 0.06_{stat} \pm 0.02_{sys}}$$

arXiv:2010.06205v1 [astro-ph.HE] 13 Oct 2020

Chinese Physics C Vol. 45, No. 2 (2021)

Science 08 Jul 2021: Vol 373, Issue 6553

ПэВатроны работают в нашей Галактике!

Cao, Z., Aharonian, F.A., An, Q. *et al.* Ultrahigh-energy photons up to 1.4 petaelectronvolts from 12 γ-ray Galactic sources. *Nature* **594,** 33–36 (2021)

Table 1 | UHE γ-ray sources

Source name	RA (°)	dec. (°)	Significance above 100 TeV (×σ)	E_{max} (PeV)	Flux at 100 TeV (CU)
LHAASO J0534+2202	83.55	22.05	17.8	0.88 ± 0.11	1.00(0.14)
LHAASO J1825-1326	276.45	−13.45	16.4	0.42 ± 0.16	3.57(0.52)
LHAASO J1839-0545	279.95	−5.75	7.7	0.21 ± 0.05	0.70(0.18)
LHAASO J1843-0338	280.75	−3.65	8.5	$0.26 - 0.10^{+0.16}$	0.73(0.17)
LHAASO J1849-0003	282.35	−0.05	10.4	0.35 ± 0.07	0.74(0.15)
LHAASO J1908+0621	287.05	6.35	17.2	0.44 ± 0.05	1.36(0.18)
LHAASO J1929+1745	292.25	17.75	7.4	$0.71 - 0.07^{+0.16}$	0.38(0.09)
LHAASO J1956+2845	299.05	28.75	7.4	0.42 ± 0.03	0.41(0.09)
LHAASO J2018+3651	304.75	36.85	10.4	0.27 ± 0.02	0.50(0.10)
LHAASO J2032+4102	308.05	41.05	10.5	1.42 ± 0.13	0.54(0.10)
LHAASO J2108+5157	317.15	51.95	8.3	0.43 ± 0.05	0.38(0.09)
LHAASO J2226+6057	336.75	60.95	13.6	0.57 ± 0.19	1.05(0.16)

Celestial coordinates (RA, dec.); statistical significance of detection above 100 TeV (calculated using a point-like template for the Crab Nebula and LHAASO J2108+5157 and 0.3° extension templates for the other sources); the corresponding differential photon fluxes at 100 TeV; and detected highest photon energies. Errors are estimated as the boundary values of the area that contains ±34.14% of events with respect to the most probable value of the event distribution. In most cases, the distribution is a Gaussian and the error is 1σ.

Где расположены источники?

Extended Data Table 2 | List of energetic astrophysical objects possibly associated with each LHAASO source

LHAASO Source	Possible Origin	Type	Distance (kpc)	Age (kyr)[a]	L_s (erg/s)[b]	Potential TeV Counterpart[c]
LHAASO J0534+2202	PSR J0534+2200	PSR	2.0	1.26	4.5×10^{38}	Crab, Crab Nebula
LHAASO J1825-1326	PSR J1826-1334	PSR	3.1 ± 0.2[d]	21.4	2.8×10^{36}	HESS J1825-137, HESS J1826-130,
	PSR J1826-1256	PSR	1.6	14.4	3.6×10^{36}	2HWC J1825-134
LHAASO J1839-0545	PSR J1837-0604	PSR	4.8	33.8	2.0×10^{36}	2HWC J1837-065, HESS J1837-069,
	PSR J1838-0537	PSR	1.3[e]	4.9	6.0×10^{36}	HESS J1841-055
LHAASO J1843-0338	SNR G28.6-0.1	SNR	9.6 ± 0.3[f]	< 2[f]	—	HESS J1843-033, HESS J1844-030, 2HWC J1844-032
LHAASO J1849-0003	PSR J1849-0001	PSR	7[g]	43.1	9.8×10^{36}	HESS J1849-000, 2HWC J1849+001
	W43	YMC	5.5[h]	—	—	
LHAASO J1908+0621	SNR G40.5-0.5	SNR	3.4[i]	$\sim 10 - 20$[j]	—	MGRO J1908+06, HESS J1908+063,
	PSR 1907+0602	PSR	2.4	19.5	2.8×10^{36}	ARGO J1907+0627, VER J1907+062,
	PSR 1907+0631	PSR	3.4	11.3	5.3×10^{35}	2HWC 1908+063
LHAASO J1929+1745	PSR J1928+1746	PSR	4.6	82.6	1.6×10^{36}	2HWC J1928+177, 2HWC J1930+188,
	PSR J1930+1852	PSR	6.2	2.9	1.2×10^{37}	HESS J1930+188, VER J1930+188
	SNR G54.1+0.3	SNR	$6.3^{+0.8}_{-0.7}$[d]	1.8 – 3.3[k]	—	
LHAASO J1956+2845	PSR J1958+2846	PSR	2.0	21.7	3.4×10^{35}	2HWC J1955+285
	SNR G66.0-0.0	SNR	2.3 ± 0.2[d]	—	—	
LHAASO J2018+3651	PSR J2021+3651	PSR	$1.8^{+1.7}_{-1.4}$[l]	17.2	3.4×10^{36}	MGRO J2019+37, VER J2019+368,
	Sh 2-104	H II/YMC	3.3 ± 0.3[m]/4.0 ± 0.5[n]	—	—	VER J2016+371
LHAASO J2032+4102	Cygnus OB2	YMC	1.40 ± 0.08[o]	—	—	TeV J2032+41
	PSR 2032+4127	PSR	1.40 ± 0.08[o]	201	1.5×10^{35}	MGRO J2031-
	SNR G79.8+1.2	SNR candidate	—	—	—	VER J2032+4
LHAASO J2108+5157	—	—	—	—	—	—
LHAASO J2226+6057	SNR G106.3+2.7	SNR	0.8[p]	~ 10[p]	—	VER J2227+608, Boomerang Nebula
	PSR J2229+6114	PSR	0.8[p]	~ 10[p]	2.2×10^{37}	

Cygnus Cocoon

Пульсары имеются в окрестностях всех источников, тогда как остатки сверхновых только в окрестностях 4 обнаруженных источников!

Это значит, что существующие модели ускорения к. л. должны быть пересмотрены!

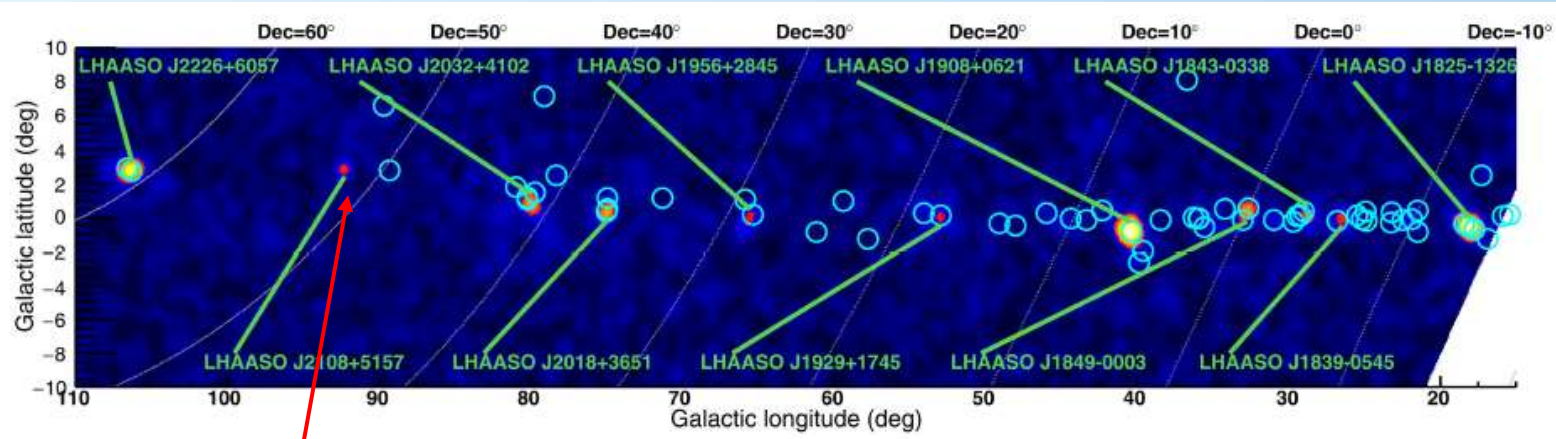

Extended Data Fig. 4 | LHAASO sky map at energies above 100 TeV. The circles indicate the positions of known very-high-energy γ-ray sources.

Most possible candidates to accelerate particles up to hundreds of TeV include SNRs, pulsar wind nebulae (PWNe), and young stellar clusters. Based on those catalogs collected by SIMBAD[2], we searched for the possible accelerators within 0.8° from the center of the LHAASO source. While there are no SNRs and PWNe counterparts, two young star clusters Kronberger 82 (Kronberger et al. 2006) and Kronberger 80 (Kharchenko et al. 2016) are found.

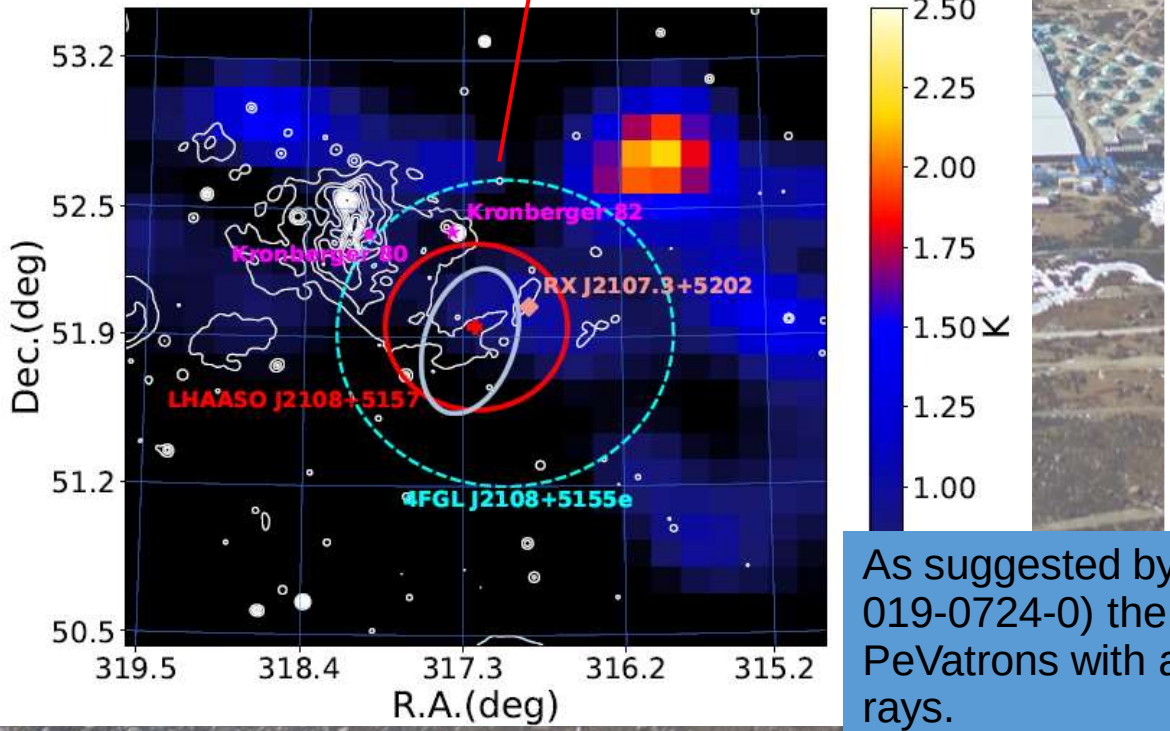

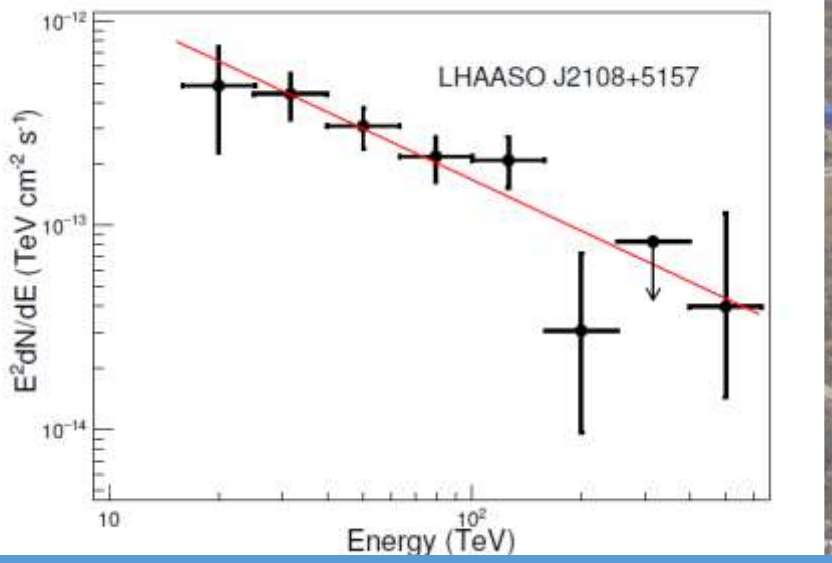

As suggested by Aharonian et al. (2019) (doi: 10.1038/s41550-019-0724-0) the young massive stars may operate as proton PeVatrons with a dominant contribution to the Galactic cosmic rays.

Примеры найденных источников: (LHAASO J0341+5258 и LHAASO J1908+0621)

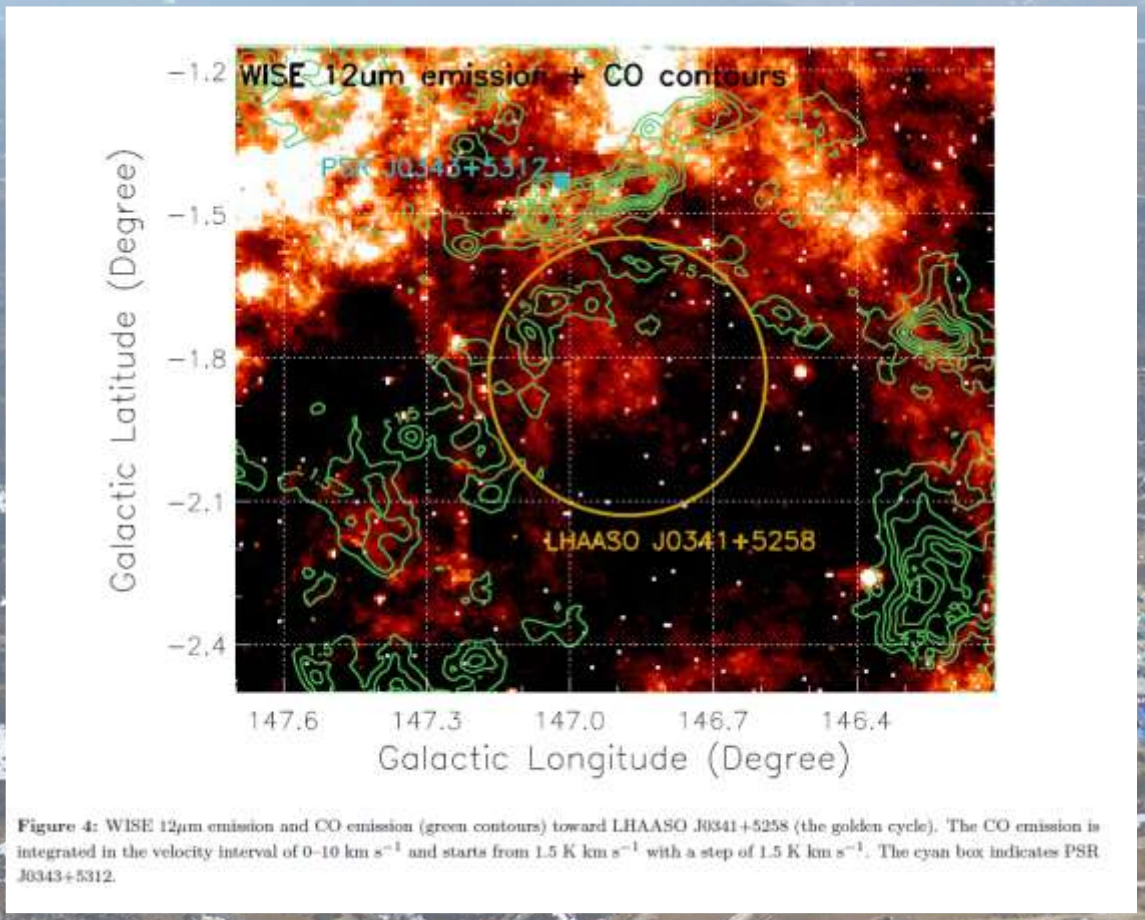

Figure 4: WISE 12μm emission and CO emission (green contours) toward LHAASO J0341+5258 (the golden cycle). The CO emission is integrated in the velocity interval of 0–10 km s^{-1} and starts from 1.5 K km s^{-1} with a step of 1.5 K km s^{-1}. The cyan box indicates PSR J0343+5312.

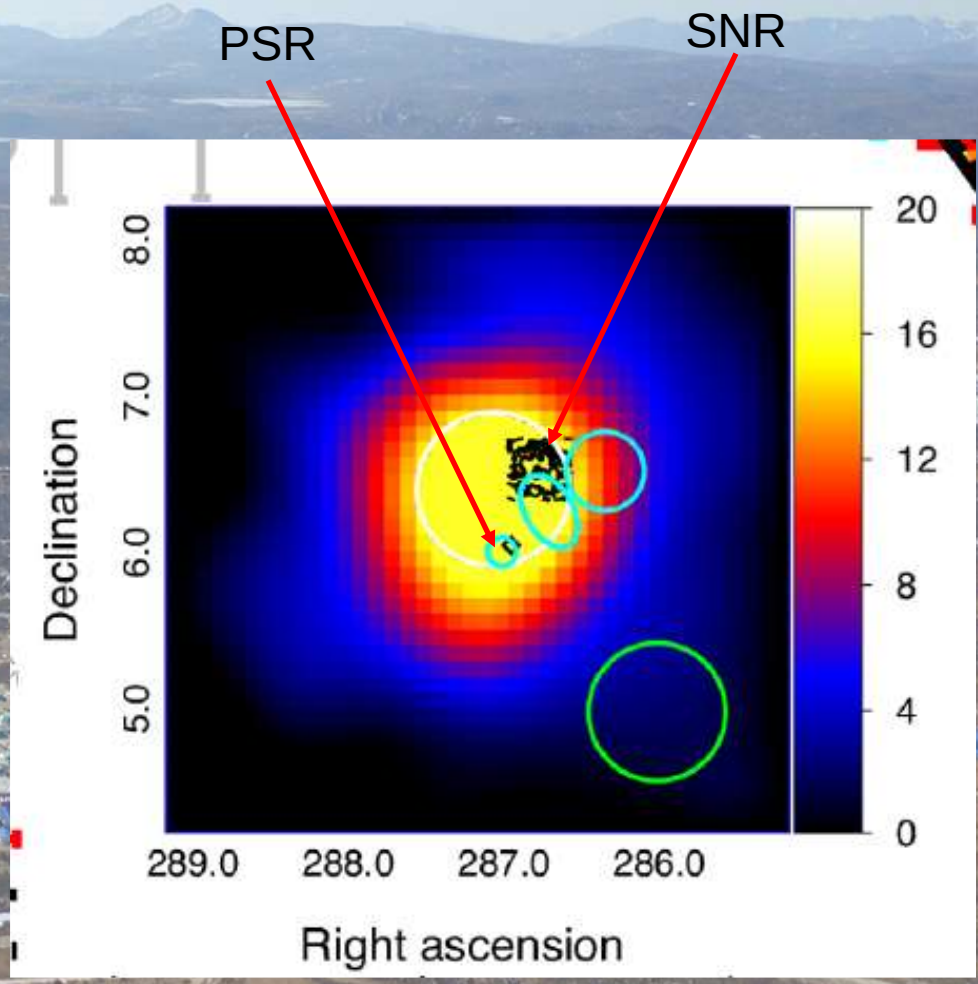

So far we cannot get any solid conclusion of the nature of LHAASO J0341+5258. No suitable candidates in the vicinity are favored to produce the VHE emissions. If the emission is produced by hadronic process, this source can also serve as a powerful cosmic ray accelerator.

Электронные или адронные ускорители работают в нашей галактике?

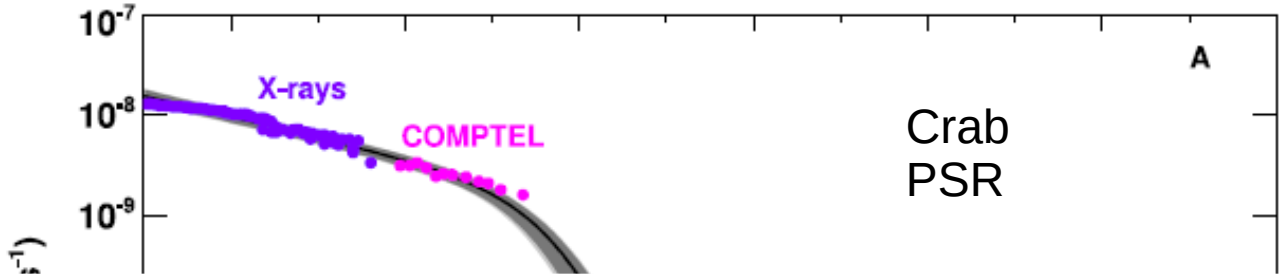

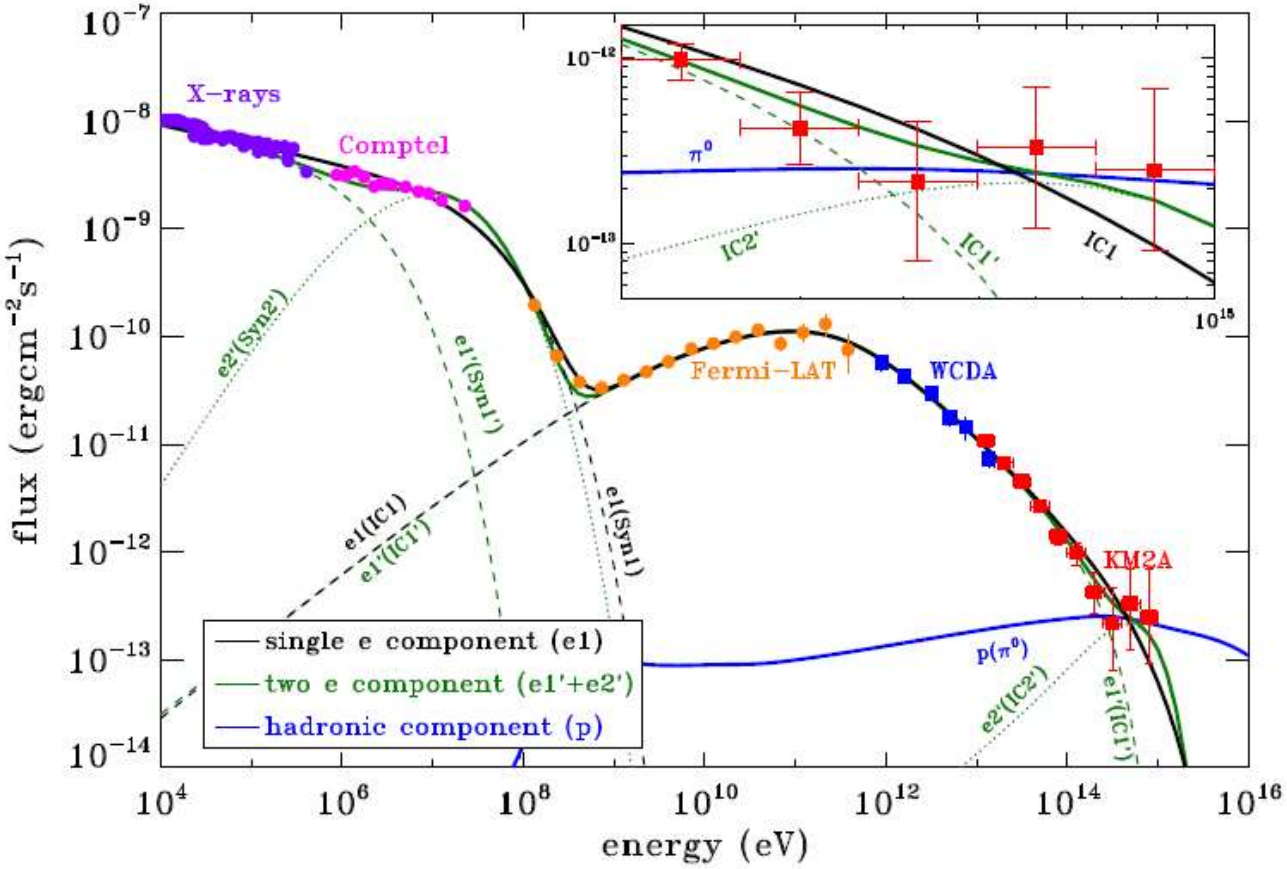

Только источник в Крабовидной туманности уверенно ассоциируется с известным пульсаром

Однако и тут не исключена примесь адроного ускорителя

Теоретикам предстоит найти новые механизмы ускорения частиц во Вселенной!

***Science* 08 Jul 2021: Vol 373, Issue 6553 pp. 425-430.**

The First LHAASO Catalog of Gamma-Ray Sources

arXiv:2305.17030v1 [astro-ph.HE] 26 May 2023

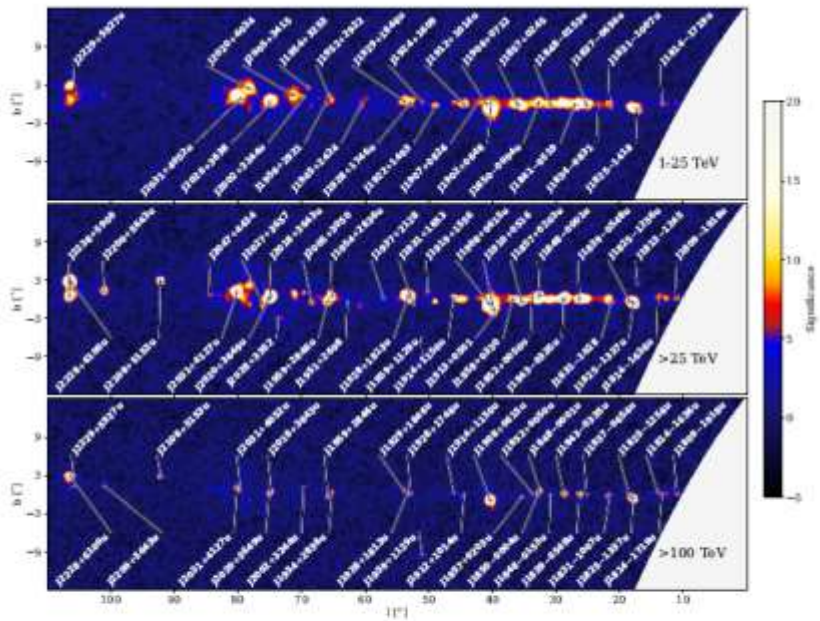

Figure 6. LHAASO significance map within region $10° \leq l \leq 115°$, $|b| \leq 12°$. Top: WCDA (1 TeV < E < 25 TeV) significance map. Middle: KM2A (E > 25 TeV) significance map. Bottom: KM2A (E > 100 TeV) significance map. In this figure and following, the LHAASO source are represented by gray crosses and white labels. The LHAASO sources, which the WCDA components are with higher significance, are plotted in top panel. The LHAASO sources, which the KM2A components are with higher significance, are plotted in middle panel. Meanwhile, the UHE source are also shown in the bottom panel.

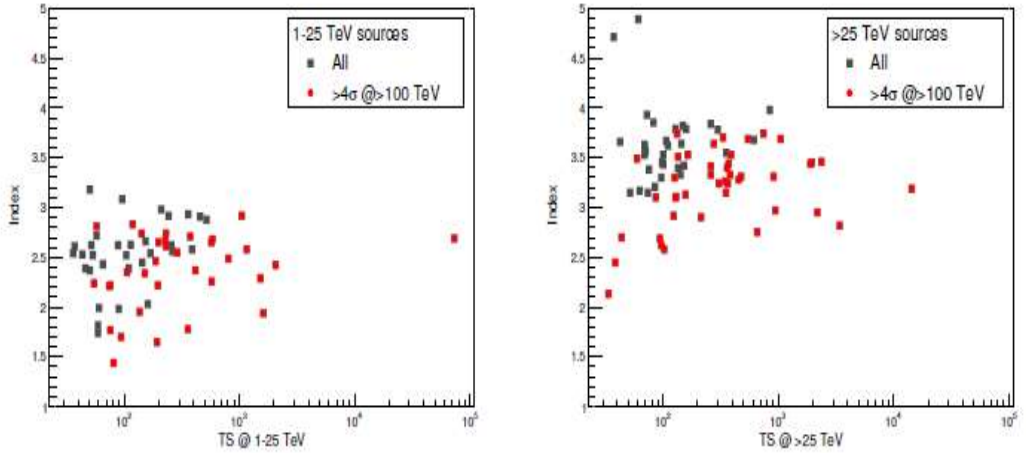

Figure 9. Distribution of the spectral index and the significance for sources at energy range from 1–25 TeV (left) and E > 25 TeV (right), respectively. The red points indicate the sources also with significance above 4σ at E >100 TeV. The extragalactic sources are excluded in these figures.

For each source, we provide its position, extension and spectral characteristics.
Furthermore, based on our source association criteria, 32 new TeV sources are proposed in this study.
Additionally, 43 sources are detected with ultra-high energy (E > 100 TeV) emission at > 4σ significance level.

Great bulk of sources are associated with Pulsars.
Seven of the new TeV sources do not have any associations.
They are tentatively classified as “dark” sources in this work.

LHAASO sources Summary

1. 43 sources are detected with ultra-high energy (E > 100 TeV) emission at > 4σ significance level.
2. В нашей галактике работают ПэВатроны!
3. Измерены энергетические спектры гамма-квантов от некоторых источников в области 0.1 – 1.5 ПэВ
4. Измеренные спектры указывают на адронную природу регистрируемых гамма-квантов (по крайней мере в некоторых источниках)
5. Это значит, что в нашей галактике работают ускорители, разгоняющие заряженные частицы (космические лучи) как минимум до 15-20 ПэВ
6. Eight out of the forty-three UHE sources are not detected at the 1-25 TeV range, representing a new class of gamma-ray sources dominated by emission above tens of TeV. Thirty-five 1LHAASO sources are associated with energetic pulsars.
7. Остатки сверхновых скорее всего не годятся в качестве источников к. л. сверхвысоких энергий. Следует искать новые механизмы ускорения к. л.

Measurement of ultra-high-energy diffuse gamma-ray emission of the Galactic plane from 10 TeV to 1 PeV with LHAASO-KM2A

arXiv:2305.05372v1 [astro-ph.HE] 9 May 2023

Difuse emissions from the inner (15 < l < 125, jbj < 5) and outer (125 < l < 235, jbj < 5) Galactic plane are detected with 29:1 and 12:7 significance, respectively. The outer Galactic plane diffuse emission is detected for the first time in the very- to ultra-high-energy domain (E > 10 TeV).

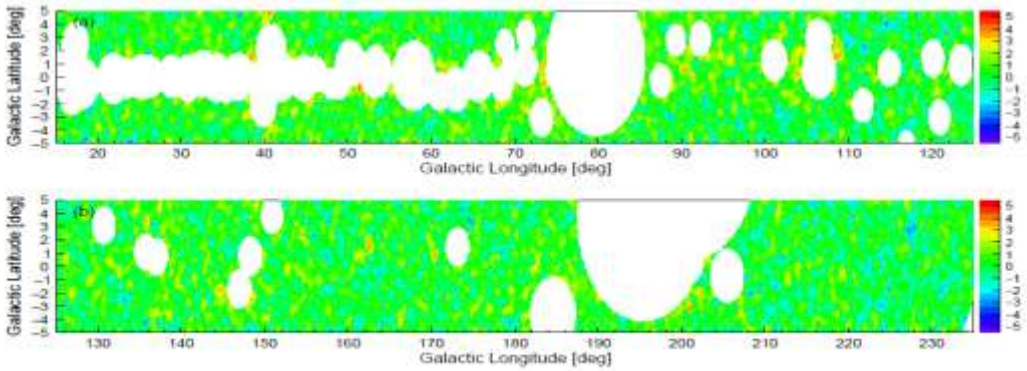

FIG. 1. The significance maps in Galactic coordinate of the inner Galaxy region (panel (a)) and outer Galaxy region (panel (b)) above 25 TeV after masking the resolved KM2A and TeVCat sources.

spectrum in the inner Galaxy regions can be described by a power-law function with an index of ~2.99, which is different from the curved spectrum as expected from hadronic interactions between locally measured cosmic rays and the line-of-sight integrated gas content. The measured flux is higher by a factor of ~3 than the prediction. A similar spectrum with an index of ~2.99 is found in the outer Galaxy region, and the absolute flux for 10<E<60 TeV is again higher than the prediction

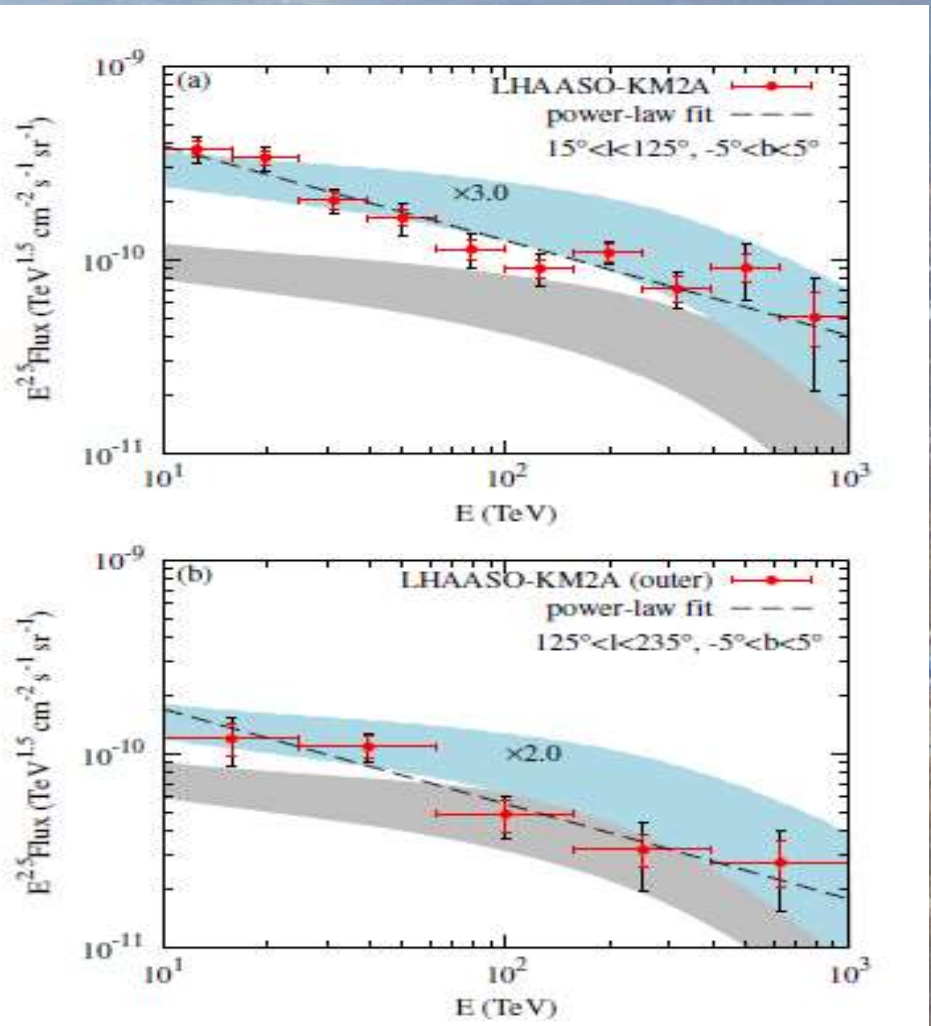

FIG. 2. Measured fluxes of diffuse γ-ray emission in the inner and outer Galaxy regions. The smaller error bars show the statistical errors and the larger ones show the quadratic sum of the statistical and systematic errors. In each panel, the dashed line shows the best-fit power-law function of the data, the grey shaded band shows the model prediction assuming local CR spectra and the gas column density with the same mask as the data, and the cyan shaded band is the grey one multiplied by a constant factor of 3.0 for the inner region and 2.0 for the outer region.

Фундаментальные результаты уже полученные LHAASO в смежных областях науки путем анализа измеренных потоков астрофизических гамма-квантов

Exploring Lorentz Invariance Violation from Ultrahigh-Energy γ Rays Observed by LHAASO.

Zhen Cao *et al.* (LHAASO Collaboration). Phys. Rev. Lett. 128, 051102 – Published 3 February 2022.

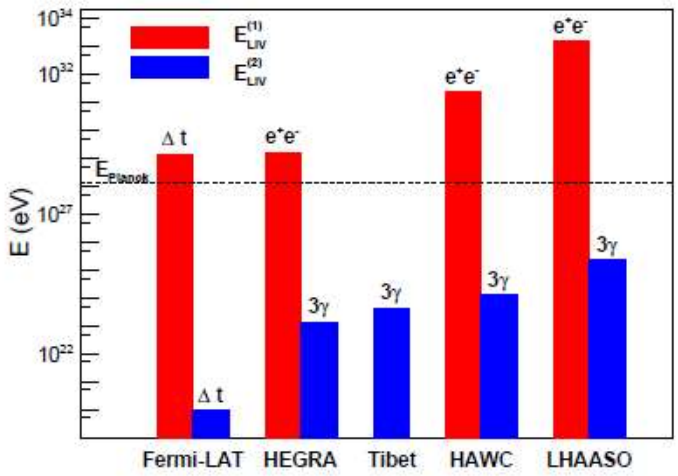

FIG. 3. Comparison of the constraints on the $E^{(1)}_{\rm LIV}$ and $E^{(2)}_{\rm LIV}$ derived from LHAASO and other experiments [11, 19, 20, 22, 40]. We show constraints due to the photon decay (e^+e^-) and the photon splitting (3γ) processes for all experiments except for Fermi-LAT which adopted the time delay method (Δt).

Constraints on heavy decaying dark matter with 570 days LHAASO observation

(arXiv:2210.15989v1 [astro-ph.HE] 28 Oct 2022)

"We find no excess of dark matter signals, and thus place some of the strongest γ-ray constraints on the lifetime of heavy dark matter particles with mass between 10^5 to $10^{9.97}$ GeV."

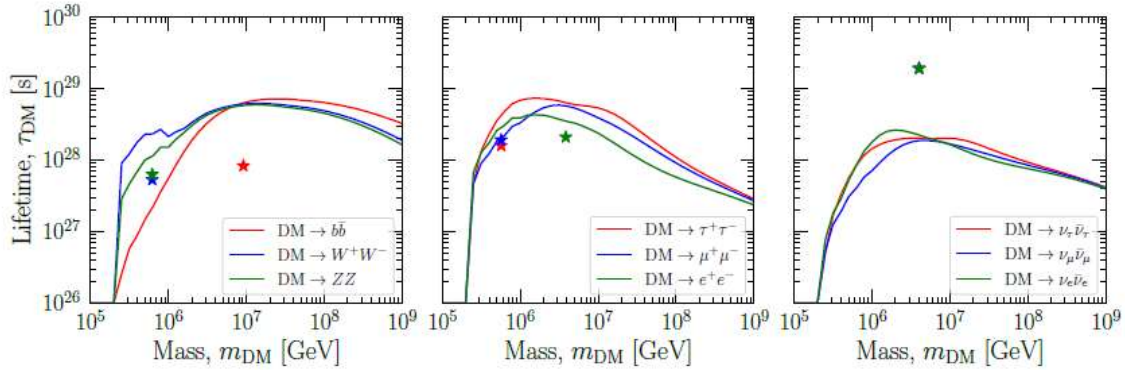

FIG. S3. Constraints at 95% CL on DM lifetime obtained with the profile likelihood analysis for the DM decay channels. The stars correspond to the best-fit scenario from the latest IceCube data [67].

The first-order LIV energy-scale is constrained to be higher than 10^5 M_{pl}, and the second-order LIV energy-scale should exceed 10^{-3} M_{pl}. (Mpl ≈ 1.22 × 10^{28} eV)

A teraelectronvolt afterglow from a narrow jet in the extremely bright GRB 221009A (LHAASO col. *Science*, to be published soon)

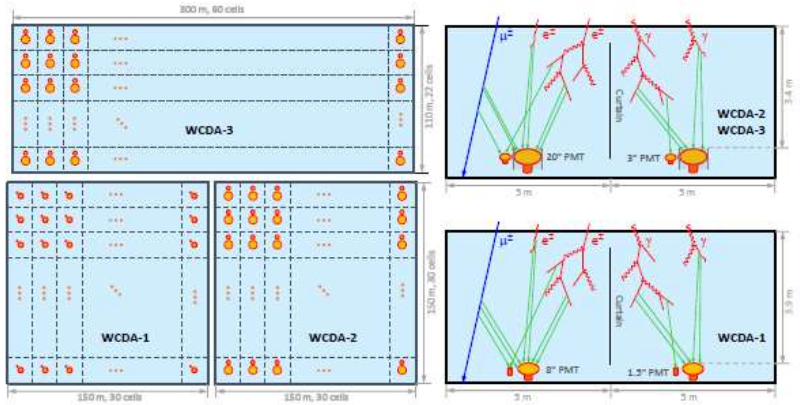

Figure 6: Layout sketch of the LHAASO-WCDA (left) and side views of two cells (right). In the left panel, two sets of circles in each cell partitioned by black dashed lines denote the big and the small PMTs, and the black dashed lines represent the plastic curtains. The water depth over the PMT top surface is 3.9 m and 3.4 m for WCDA-1 and WCDA-2 & 3, respectively.

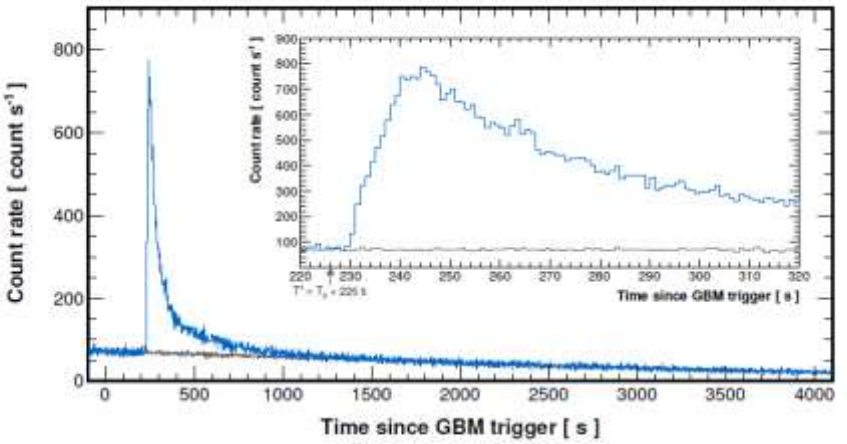

Figure 1: Count-rate light curve (in blue color) of GRB 221009A with $N_{\rm hit} \geq 30$ (energy range 0.2–7 TeV, $N_{\rm nhit}$ is the equivalent number of fired detector cells) detected by LHAASO-WCDA within the angular radius $\sim 3.0^{\circ}$. The inset panel shows the zoomed-in view during 220–320 s after the GBM trigger (T_0) and the arrow indicates the new reference time $T^* = T_0 + 226$ s for the further light curve analysis (see the text for more details). The dark black lines in both panels show the background rates.

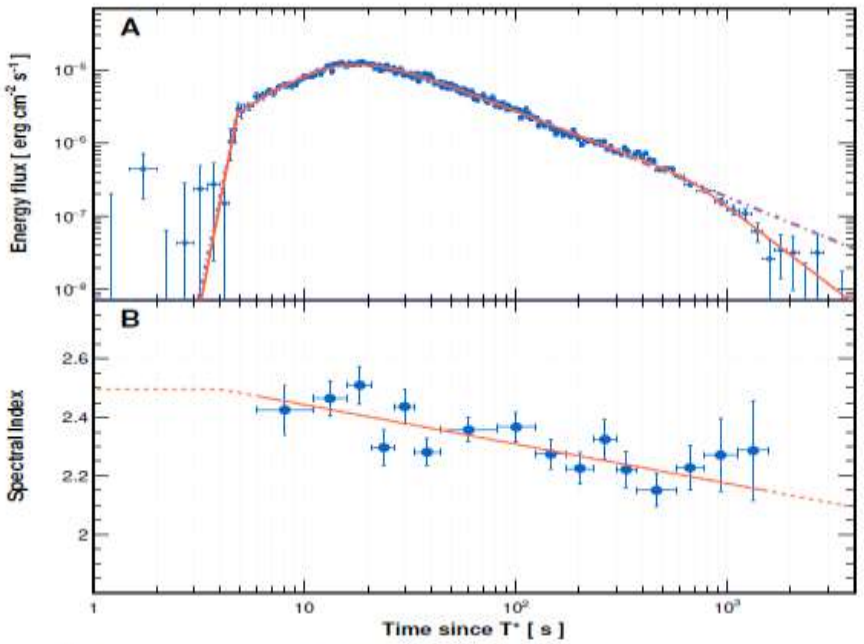

Figure 3: Light curve of energy flux and spectral evolution in the VHE band for GRB 221009A. Panel A: the light curve of energy flux integrated over 0.3–5 TeV, where the solid orange curve is the fitting function consisting of four joint power laws to describe the four-segment features in the light curve: *rapid rise*, *normal rise*, *normal decay*, and *steep decay*. The dash-dotted line in dark purple represents the fitting function assuming one segment for the whole decay phase. Some data points that non-statistically deviate from the fitted line (solid orange curve) are supposed to owning to influence from the GRB flares. Panel B: temporal evolution of the power-law spectral index (the blue circles) of VHE photons, determined from time-resolved intrinsic spectra. Note that the spectral index γ employed for the light curve calculation at time t is obtained from the function $\gamma(t) = a\log(t = T - T^*) + b$ (the orange line) that fits the data points. In application, the index is considered to be flat before $T_0 + 230$ s when no TeV signal was detected.

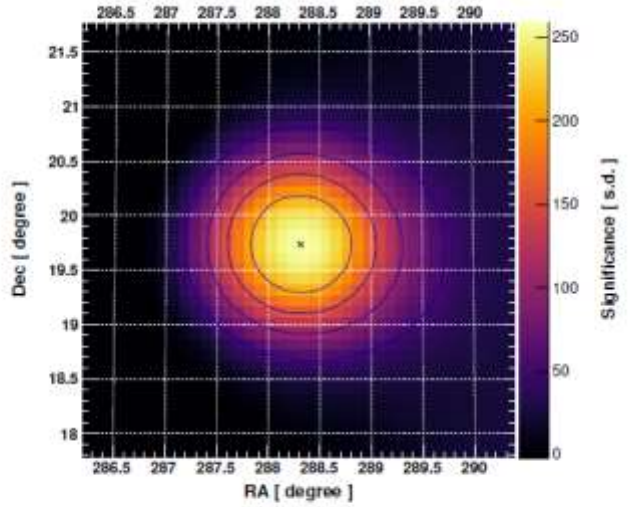

Figure 9: Significance map of the GRB emissions detected by LHAASO-WCDA. Reconstructed events with $N_{\rm hit} \geq 30$ as the baseline event selection criterion are analyzed. The cross in the center of the map is the fitted position of the burst, and the blue lines are contour levels separated by 1/5 of the maximum significance.

A structured jet explains the extreme GRB 221009A

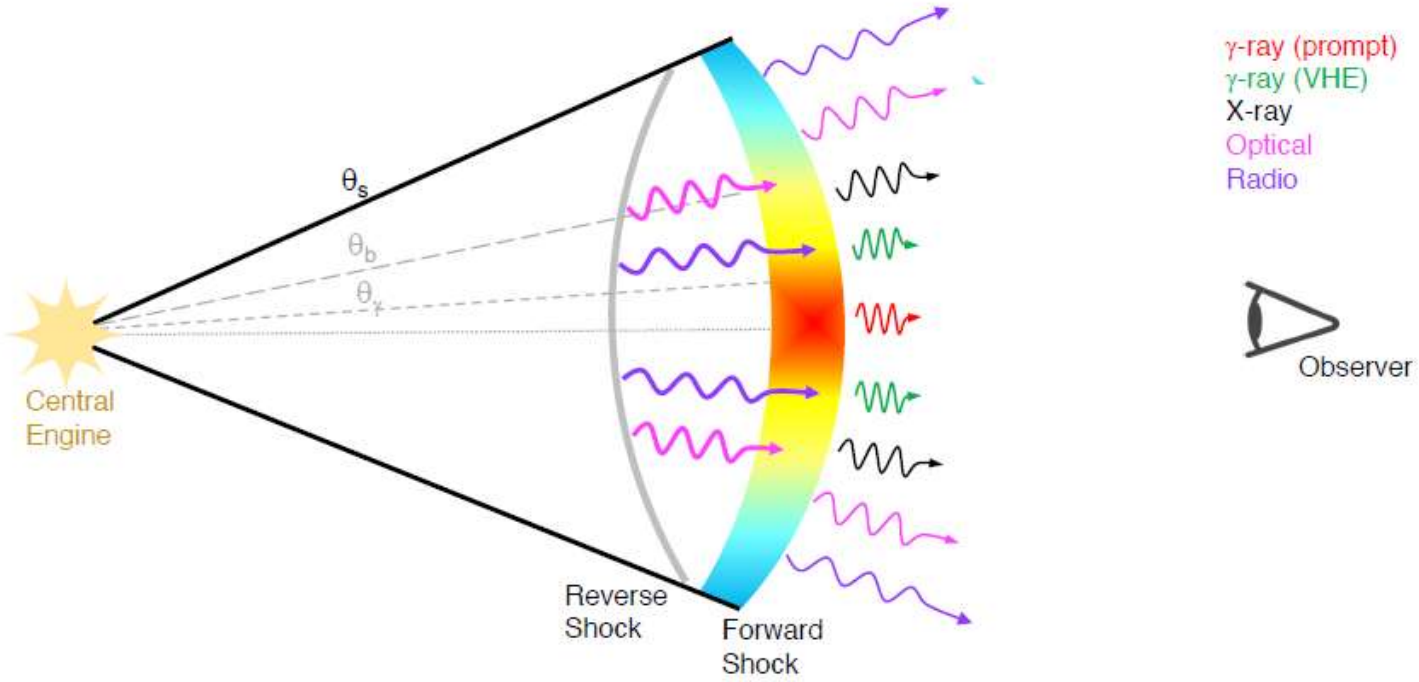

Figure 3: **Schematic of the structured jet for GRB 221009A.** Emission from the forward and reverse shocks are produced by the jet out to its truncation angle θ_s. The angular structure of the jet, $dE_K/d\Omega \propto \theta^{-a}$, breaks slightly at θ_b, transitioning from a slope $a_1 \sim 0.75$ to $a_2 \sim 1.15$. The prompt gamma-rays may be radiated from the central narrow core of aperture θ_γ.

arXiv:2302.07906v1 [astro-ph.HE] 15 Feb 2023

A Large Cosmic Ray Bubble in the Cygnus-X Region

LHAASO col. *Nature*, in press

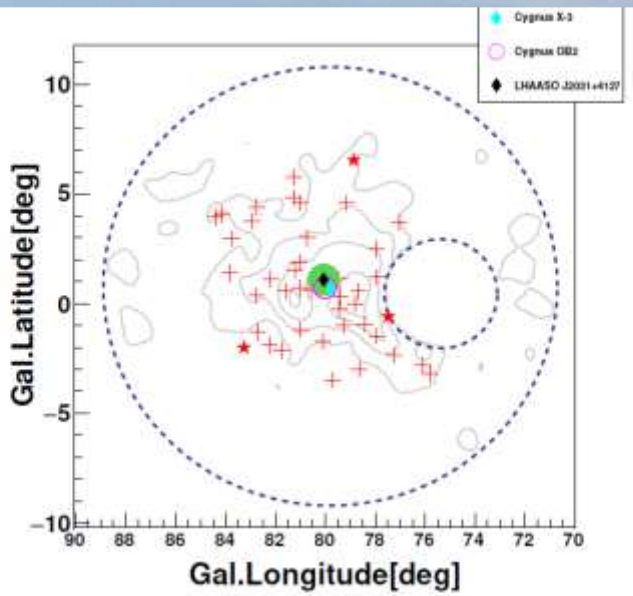

Figure 1: Photon distribution in the Cygnus-X region. The significance map of γ-rays from 25 TeV to 100TeV of the bubble is shown by grey contours starting from 3σ with a step of 3σ. This structure is about 20° in longitude and 15° in latitude. The black diamond located at the centre of the γ-ray image marks LHAASO J2031 + 4127 (RA=307.95°±0.02°, DEC=41.46°±0.02°), which coincides with the unidentified source TeV 2031+4130 [7]. There are 42 photon-like events within a radius of 6 degree with an estimated background of 10.34. Three events with energy above 1 PeV are marked with stars and the other 39 events are marked with pluses. The photons above 400 TeV extend beyond 6°, but with a higher CR background contamination, so it is not practical to show them individually on the map. In addition, seven more such high energy photons, 2 of them with energy above 1 PeV, are located in the region of radius of 0.7° relative to the centre dubbed *core* (filled green circle). Possible contamination of the CR background is 0.74 events. The core region contains at least three interesting objects - Cygnus OB2 (red circle), Cyg X-3 (cyan diamond) and a pulsar, and their contribution to the observed high energy emission is beyond the scope of this paper. The larger circle in blue dotted line represents the ROI used in this study, while the smaller circle in blue dotted line marks the unidentified source LHAASO 2018+3651 which is masked in the analysis.

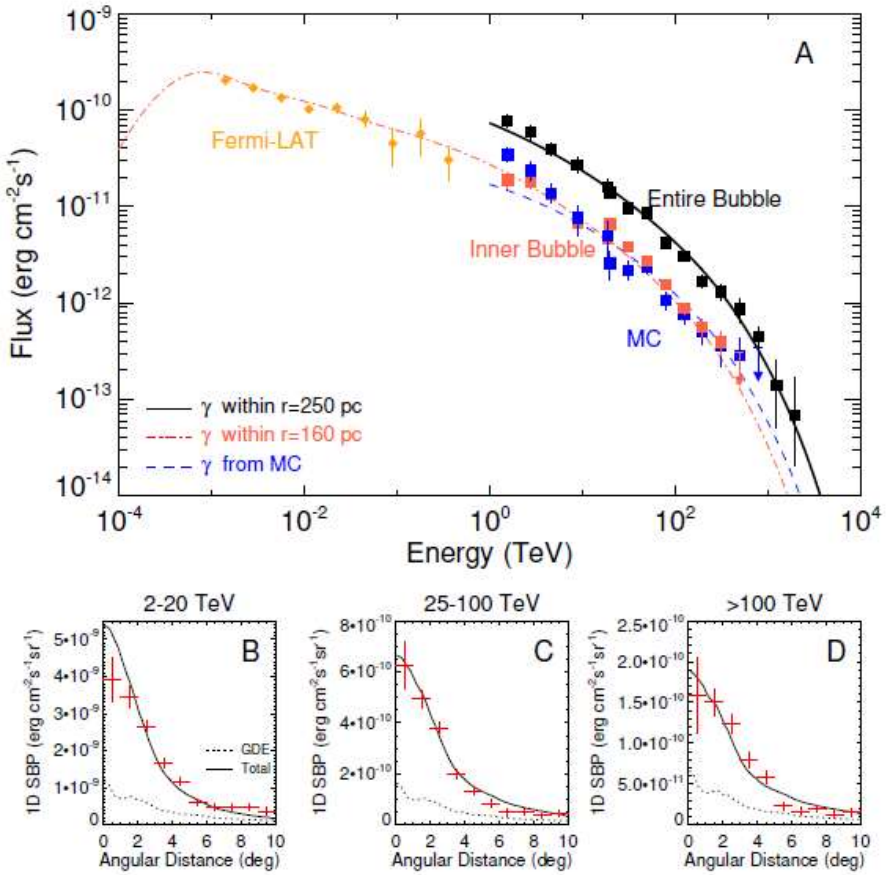

Figure 4: Modeling of the Cygnus Bubble that simultaneously fits the SEDs and 1-dimensional intensity profiles of γ-rays. In panel A, the measured fluxes from the entire bubble (black) and the inner bubble (red) are shown. The proton injection luminosity is $L_p = 1.1 \times 10^{37}$erg/s with the acceleration spectrum $E_p^{-2.3}\exp(-E_p/3\,\mathrm{PeV})$. The diffusion coefficient is $D(E_p) = 1.8 \times 10^{26}(E_p/1\mathrm{TeV})^{0.7}$ cm^{2}s^{-1}. The blue dashed curve shows the emission of protons inside MCs. Black squares show the total fluxes measured by LHAASO. Blue squares are the flux associated with the MC distribution in the entire bubble region measured by KM2A. Orange diamonds present the flux of the Cygnus Cocoon measured by Fermi-LAT [1].The black solid, red dot-dashed, and blue dashed curves show emissions within 250 pc, 160 pc of the CR source and inside MCs, respectively. Panels B, C, D show the measured surface brightness profile in the energy ranges of $2-20$ TeV, $25-100$ TeV and >100 TeV (red crosses), in comparison with the model prediction (black curves). Dotted curves show the expected contribution of GDE. See Supplementary Material for details of the model.

ENDA (Electron-Neutron detector Array)

Задача – измерение энергетического спектра и массового состава к. л. в области 1-100 ПэВ (программа минимум), а затем в области выше 100 ПэВ (ENDA-400)

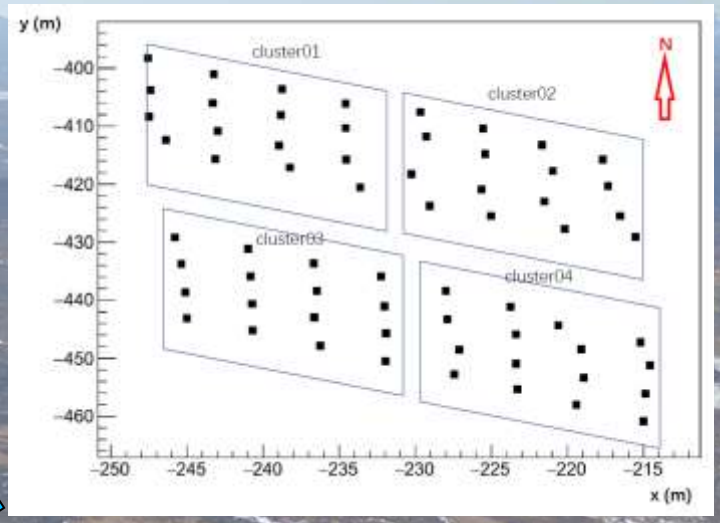

ENDA-64

64 детектора установлены, идет настройка и отладка

Заключение

1. Эксперимент LHAASO не имеет аналогов и вряд ли у него появятся конкуренты в ближайшие годы.

2. Даже при работе лишь части установок там уже были получены выдающиеся результаты.

3. В ближайшее время стоит ожидать новых открытий в различных областях знаний – в астрофизике, в астрономии, в космологии, в физики космических лучей, в поиске темной материи и т. д.

4. Участие российских ученых из ИЯИ РАН в этом эксперименте класса Mega-Science со своей установкой (ENDA) имеет принципиальное значение и нуждается во всесторонней поддержке.


LHAASO
高海拔宇宙线观测站
Спасибо за внимание!
Стенькин Ю.В.
Зацепинские чтения 2023